

Flow Characterization of Inclined Jet in Cross Flow for Thin Film Cooling via Large Eddy Simulation

Naqavi, I.Z.¹, Savory, E.² and Martinuzzi, R. J.³

^{1,2}*The Univ. of Western Ontario, Dept. of Mech. And Materials Engg.*

³*University of Calgary, Dept. of Mech. And Manuf. Engg.*

¹ inaqavi@uwo.ca, ² esavory@eng.uwo.ca, ³ rmartinu@ucalgary.ca

Abstract

Large Eddy Simulation of inclined cylindrical jets in a cross-stream, typical for thin film cooling, is used to study the interaction between a jet and a cross flow. Simulations are performed at $Re_D=3500$ and a jet blowing ratio (*Jet Vel./Crossflow Vel.*) of 1 inclined at 30° from the wall in the stream-wise direction. Instantaneous and average vorticity fields are studied to understand the flow. The three-dimensional unsteady coherent structures are extracted from the flow show that the stream-wise vortices from the upstream turbulent flow interact with the hairpin structures of the jet.

Introduction

In modern gas turbines, high inlet flow temperatures are used to achieve higher thermal efficiencies and power. To avoid the associated turbine blade failures, improved blade material properties and effective blade-cooling strategies are imperative. Thin film cooling is often employed for the first stage turbine blades. In this approach, cooling fluid is injected from rows of holes on the blade surface at an angle into the heated cross flow. The cross flow spreads the jet on the blade surface and a film of cooling fluid is formed between hot main flow and the blade.

While the mass flow coming from the jets is typically only 3-5% of the main stream, it can have a significant aerodynamic influence. The stability and effectiveness of the cooling film, in terms of providing a reliable insulating layer, are affected by the external cross flow, the film-cooling hole (nozzle) geometry, the inclination and orientation angle of the jet and the external stream turbulence. To ensure effective film cooling and minimum aerodynamic loss, it is essential to understand the flow physics governing the interaction between the inclined jet and the cross flow.

Numerous experimental studies of the heat transfer, flow field and jet discharge coefficient i.e. ratio of actual mass flow and ideal mass flow from jet exist (cf. Sargison et al. [1], Lee et al. [2], Rowbury et al. [3] and Gritsch et al. [4]). However, inherent limitations in spatial and temporal resolution have motivated several numerical simulation studies to investigate the flow physics in greater detail. Most of those simulations have been done using Reynolds-Averaged Navier-Stokes (RANS) equations. Lakehal et al [5] calculated the temperature and velocity field, using standard and two-layer $k-\varepsilon$ models. They were able to predict the jet span-wise spreading reasonably well but not the wall normal spreading. Acharya et al. [6] performed RANS calculations with an array of turbulence models and found that the vertical spreading rate of the jet was over predicted while the lateral was under predicted. Medic and Durbin [7] performed RANS calculations for film cooling on actual turbine blade geometries. They found that by restricting spurious turbulence energy production by the turbulence model, better

agreement between the experimental and numerical results for heat transfer coefficient is achievable. In all of these numerical studies, the results are unreliable since ad-hoc modifications of the turbulence models were needed to match prediction and observation. Furthermore, these simulations do not provide information about the fundamental interaction between jets and cross-stream. Recently Tyagi and Acharya [8] performed Large Eddy Simulation (LES) for thin film cooling at moderately higher Reynolds numbers (11,100 and 22,200) and achieved much better agreement with experimental results for velocity and cooling effectiveness. They also showed the underlying flow structures and their effect on heat transfer. They identified hairpin vortices as being the principal jet structure.

The main goal of the present work is to understand the physics of an inclined jet interaction in a cross flow using Large Eddy Simulation with a realistic turbulent field. Here, an inclined jet is introduced in a channel flow with fully developed turbulence. It will be shown that the upstream turbulence has a significant effect on the evolution of the jet, which will greatly influence the film cooling.

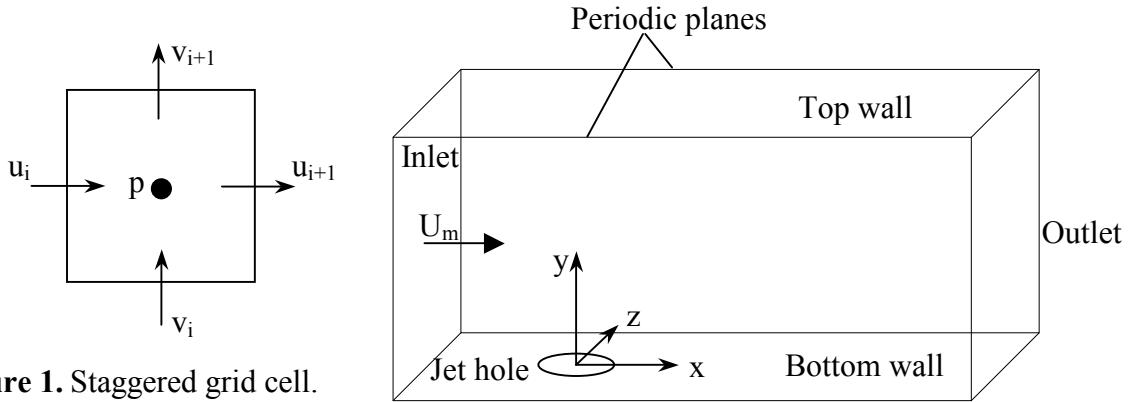


Figure 1. Staggered grid cell.

Figure 2. Schematic of computational domain.

Mathematical Model and Numerical Method

In LES, the governing equations for the conservation of mass and momentum are spatially filtered [9], with the filter width proportional to the grid size in the computational domain. The resulting non-dimensional equations are:

$$\frac{\partial U_i}{\partial x_i} = 0 \quad (\text{conservation of mass})$$

$$\frac{\partial U_i}{\partial t} + \frac{\partial U_i U_j}{\partial x_j} = -\frac{\partial p}{\partial x_i} + \frac{1}{\text{Re}_D} \frac{\partial^2 U_i}{\partial x_j^2} - \frac{\partial \tau_{ij}}{\partial x_j} \quad (\text{conservation of momentum}),$$

where U_i is the filtered velocity field and the repeated indices imply summation over the three coordinate directions. The velocities are non-dimensionalized with the mean mid

height channel velocity U_m at the inlet of the cross flow. All the lengths are non-dimensionalized with the jet hole diameter D . The Reynolds number is defined as $Re_D = U_m D / \nu$, where ν is the kinematic viscosity of the fluid. Also, p is the pressure, non-dimensionalized by the product of the density ρ and U_m^2 .

The term τ_{ij} represents the sub-grid scale (SGS) stress tensor. SGS represent the irresolvable scale of the flow, which has to be modeled. In this study, a dynamic mixed model (DMM) is used to model the SGS stress tensor (Zang et al. [10]).

A fractional step scheme [9] is used to solve the momentum equations on a staggered grid (Figure 1), where the velocities are defined on the cell walls and the pressure at the cell centre. In this method a second order semi-implicit time advancement scheme is used where convection terms are discretized explicitly with a third order Runge-Kutta method and diffusion terms are discretized implicitly with a Crank-Nicolson scheme. All the spatial derivatives are approximated with a second order central difference scheme. The resulting system of linear equations is approximately factorized and solved with a Tri-Diagonal Matrix Algorithm (TDMA). In the pressure-Poisson equation, the Laplacian is discretized with a second order central difference scheme. Using the fact that span-wise direction is periodic, Fourier decomposition is applied in that direction and the resulting systems of equations are solved with a cyclic reduction scheme [11], which is implemented through FISHPAK subroutines.

The physical domain is shown in figure 2. At the bottom plate, the outlet of the inclined circular jet appears as an elliptical hole. The center of the coordinate system is aligned with the center of the hole, which lies $5D$ downstream from the inlet plane and at the center in the span wise direction. The x-axis is aligned with the stream-wise direction, the y-axis with the wall normal direction and the z-axis with the span wise direction. The domain has the dimensions of $17D$, $7.5D$ and $6D$ (or $[-5D, 12D] \times [0, 7.5D] \times [-3D, 3D]$) in the x, y and z directions, respectively. The cross-flow inlet is at the left hand plane and at the right hand side there is the outflow plane. Top and bottom are solid walls. The domain walls in the z-directions are the periodic planes. The domain is discretized with $171 \times 71 \times 64$ (x,y,z) grid points. The grid spacing in the x and z directions is uniform, while in the y direction, the grid is clustered near the top and bottom walls.

At the jet inlet, a velocity profile based on a $1/7^{\text{th}}$ law at an angle of 30 degree with respect to the stream-wise direction is imposed. The top and bottom planes satisfy the no slip conditions. Tyagi and Acharya [8] and Yuan et al. [12] in their simulation used a prescribed velocity field with an over-laid random fluctuation as inlet boundary conditions. Such boundary conditions lack actual turbulent correlations and there are no near wall structures upstream of the jet in their simulations. The most important aspect of this computation is the fully developed turbulent flow velocity specification at the inlet. For this purpose a separate channel flow code is run and the velocity profiles at a plane are saved at each time step, for several flow through times. The time step for standard

channel flow simulation is not the same as this simulation and so linear interpolation is used to calculate velocities at any given time from saved velocity data. This boundary condition will provide near wall structures, which will be obvious in the results. At the outlet plane a non-reflecting radiative boundary condition [13] is used. This simulation is run at $Re_D=3500$ with a blowing ratio of 1.

The simulation is initiated with a uniform flow field with prescribed inlet velocities for the jet and at the inlet plane, without using a turbulence model. After running the code for a non-dimensional time period of $t=20$ a solenoidal flow field is saved and the program is restarted with the turbulence model. At the inlet plane the velocities from the fully developed channel flow simulation are prescribed and the code is run for another $t=50$. After that, the velocity field is saved for every 2 non-dimensional time units and, at some specified planes, time averages are calculated and stored for next $t=100$ non-dimensional time units for subsequent analysis. Since the time step for this simulation is $\Delta t = 0.02$, based on stability criteria, in $t=100$ there are 5000 time steps which can give reasonable time-averaged values.

Results and Discussion

First, the time-average vorticity fields will be discussed as validation to show that the present results are consistent with the classical physical description of jets in a cross-flow. The counter rotating vortex pair CVP is the most commonly discussed structure associated with jets in a cross-flow. Subsequently, the instantaneous vorticity field will be presented. Finally, coherent structures will be used to describe the instantaneous picture and its relevance to the average behaviour of the jets in cross-flow.

Average vorticity field

A normal jet in a cross flow (JICF), which can be considered a specific case of an inclined jet in a cross flow, has been studied extensively. When a jet is introduced in a cross-stream it creates an intense three-dimensional coherent structures. The jet shear layer vortices, the horseshoe vortices, the counter rotating vortex pair (CVP) and wake vortices are four major structures, which have been identified. However, the origin of these structures is still a matter of debate. Of these vortices, the horseshoe vortex and CVP are quasi-steady structures and one can expect to observe these structures in time averaged flow fields.

The vorticity field is often useful for detecting the vortical structures. In figure 3, the mean span-wise vorticity ω_z is shown for the central x-y plane of the jet. There is no horseshoe vortex upstream of the jet. In normal JICF, the jet results in a sufficiently strong pressure gradient to cause boundary layer separation and formation of a horseshoe vortex. For the inclined jet, the pressure gradient is too weak to cause a horseshoe vortex.

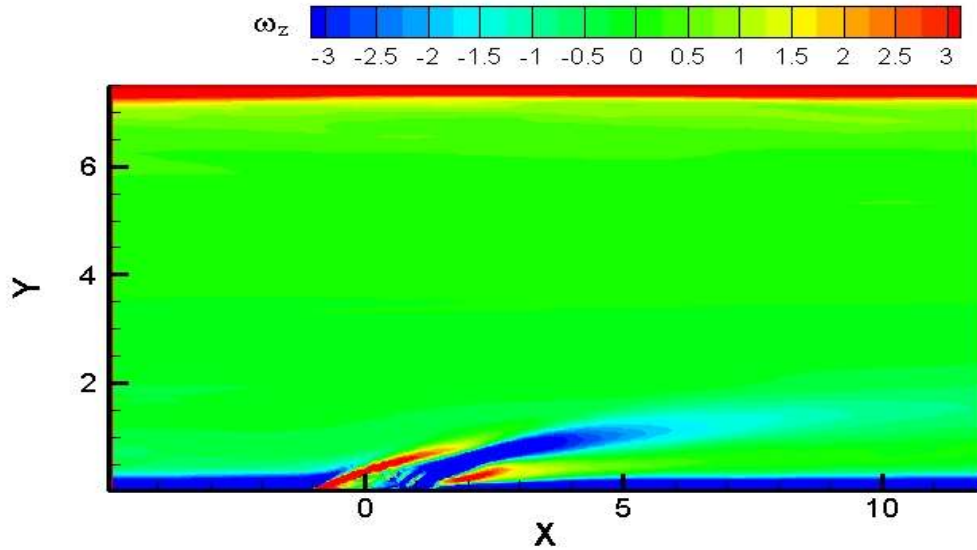


Figure 3. Average span-wise vorticity at the central x-y plane.

However, there is a jet shear layer, which penetrates into the cross-flow. The shear layer curvature indicates that jet fluid acquires stream-wise momentum from the cross-flow and follows a lower trajectory. The vorticity in the jet is generated along the wall of the delivery tube, On the upstream side, the incoming cross-flow mixes with the jet and dissipates the vorticity, but on downstream side, because of the low pressure and low mixing with the cross-flow, the jet maintains its vorticity far down stream.

The average wall normal vorticity ω_y in figure 4 shows the shear layer development around the jet. It looks similar to the flow over a cylinder except there is no vortex shedding. The main stream moves around the jet and results in the shear layer shown here.

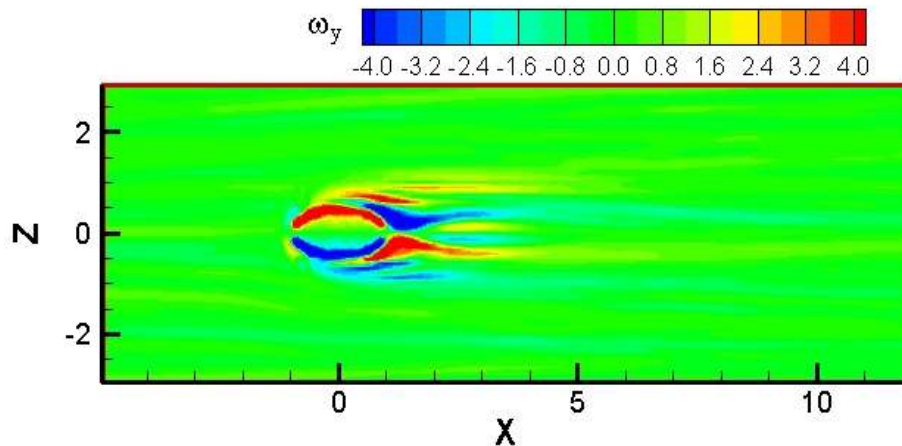


Figure 4. Average wall normal vorticity at the bottom x-z plane.

In figures 5, the average stream-wise vorticity is shown in y-z planes at different stream-wise locations. In Figure 6, the CVP can be clearly recognized from the sectional

streamlines drawn over the vorticity contours. Note that peak vorticity value decays along the flow. The growth of secondary structure near the wall because of CVP is also seen (Yuan et. al. [12]).

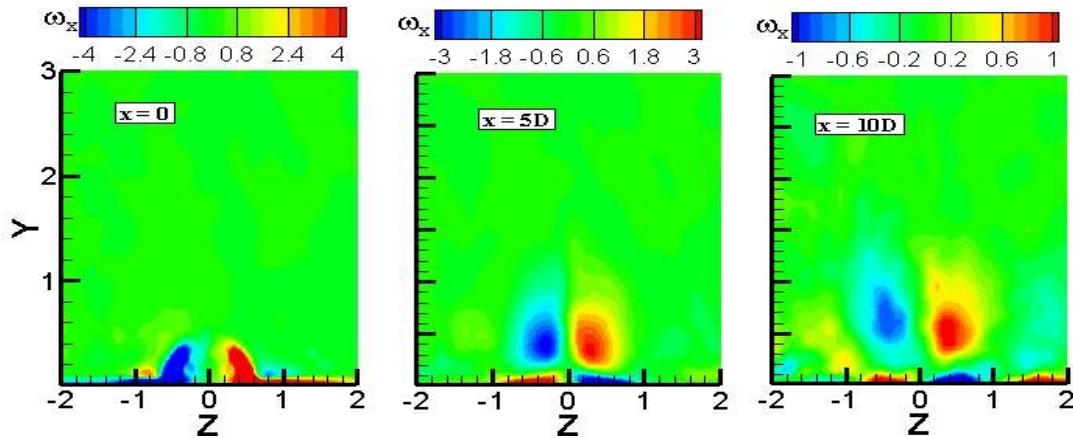


Figure 5. Average stream-wise vorticity at different y-z planes.

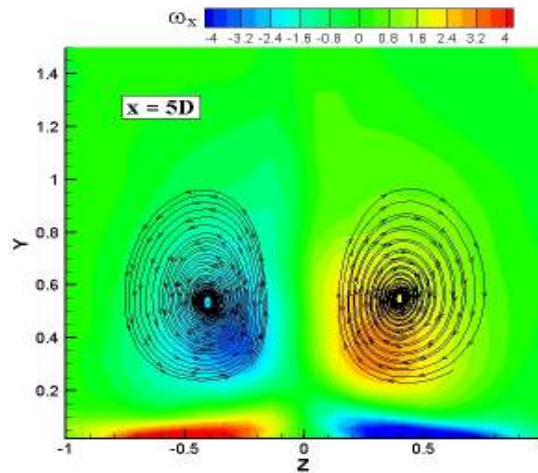


Figure 6. Streamlines overlaid on average stream-wise vorticity on y-z plane at $x = 5D$ showing CVP.

Instantaneous vorticity field

Instantaneous vorticity fields show a very complex picture. The span-wise vorticity at the central plane (figure 7) shows that the jet shear layers extend almost $2D$ downstream before breaking down. For the normal JICF, Yuan et al. [12] describes a similar behaviour, noting that the shear layers roll-up to form counter-rotating spanwise roller vortices due to Kelvin-Helmholtz instabilities. But for an inclined jet there is a remarkable difference in that roller vortices do not form along the windward shear layer, but rather only along the leeward layer. These roller structures are quite energetic, and they move farther downstream and form the upper boundary of the jet and the time averaging results in a kind of shear layer as shown in figure 3. Apart from this main roller structures there are some other smaller structures randomly dispersed in the downstream region. It will be shown later that the upstream turbulence is contributing to these structures.

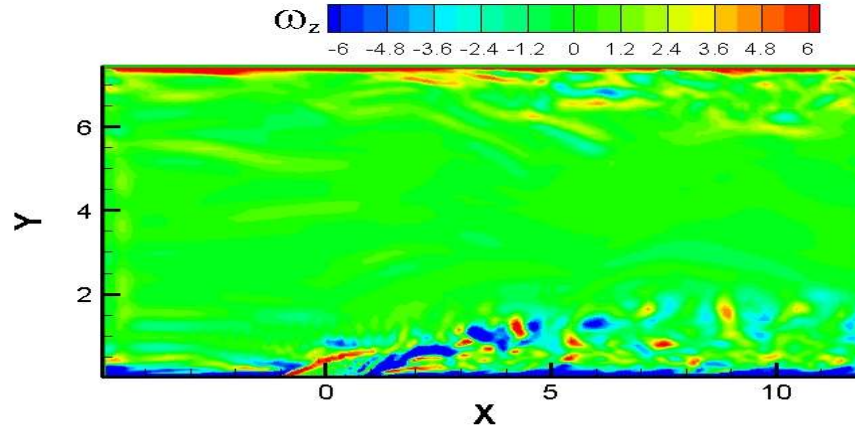


Figure 7. Instantaneous span-wise vorticity at the central x-y plane.

Wall normal vorticity (figure 8) represents the effect of cross flow turbulence. Since in this simulation the true inlet turbulent flow field is described, stream-wise wall structures are generated near the wall. These structures interact with the jet; some structures move closer to the jet and are trapped, while some move away from the jet region. Wall normal vorticity shows two distinct types of structures: one coming from upstream which are longer and one in the wake region of the jet. Fric and Roshko [14] described similar wake vortices, extending from wall to jet. However, the average vorticity field does not show these features. We will show later that these vorticities are not just random occurrences but part of organized flow behaviour in the jet.

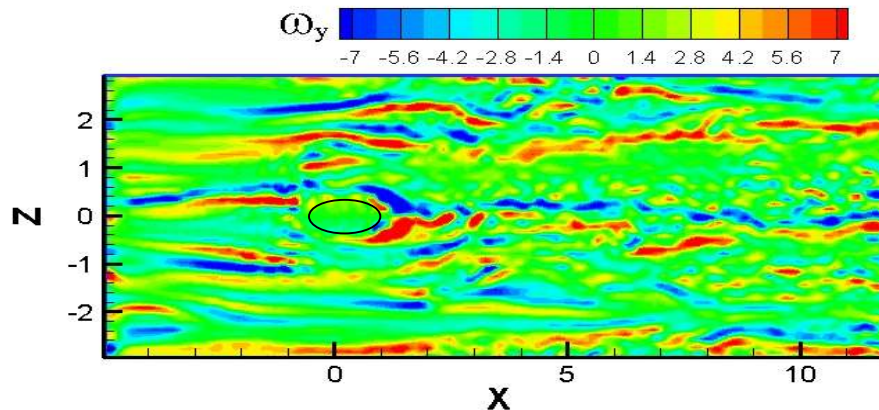


Figure 8. Instantaneous wall normal vorticity at the x-z ground plane.

In figure 9, the instantaneous stream-wise vorticity is shown at different y-z planes in the wake region. An important observation is that in the instantaneous field the CVP is not apparent. At $x = 5D$, for example, only a part of the CVP is visible near the center. It has been demonstrated that other structures are related to turbulent cross flow. While discussing the stream-wise time-averaged vorticity it was observed that the vorticity decreased along the flow direction. In the instantaneous picture, the peak vorticity strength in any given plane does not decrease along the flow, although this doesn't mean that the vorticity in jet is not decaying. Actually, the region of the jet has a steady decay in vorticity strength but the stream-wise vortices from the cross flow do not decay. On the other hand, stream-wise vortices appear randomly with opposite signs at any given plane

and by time-averaging they simply disappear from the picture and the only persistent vorticity is that belonging to jet, which decays along the flow direction.

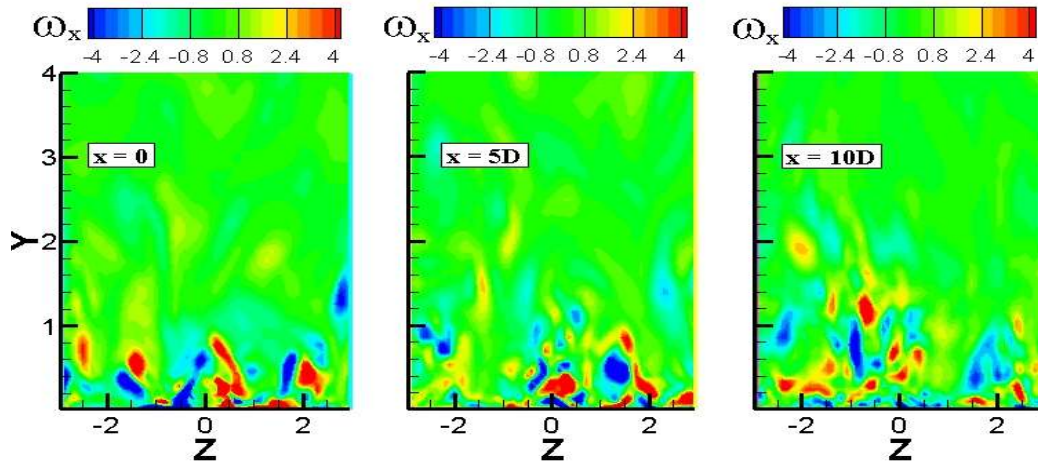


Figure 9. Instantaneous stream-wise vorticity at different y - z planes.

Coherent structures

In the previous sections, the vorticity field indicated a complex interaction between the inclined jet and the cross flow. To better understand these interactions, the stream-wise evolution of these structures needs to be investigated. The vortical structures can be deduced by observing that the vortex core represents high vorticity and a local pressure minimum. These properties can be used to extract vortical structures using the positive iso-surfaces of the Hessian or Laplacian of the pressure i.e. $p_{,ii}$, where, for incompressible flows, $p_{,ii} = (\omega_i \omega_i)/2 - S_{ij} S_{ij}$ and is related to the second invariant of the velocity gradient tensor. To give a simplified description of coherent structures involved in this flow, first a laminar flow case is considered. The corresponding iso-surfaces of $p_{,ii}$ are extracted as shown in figure 10.

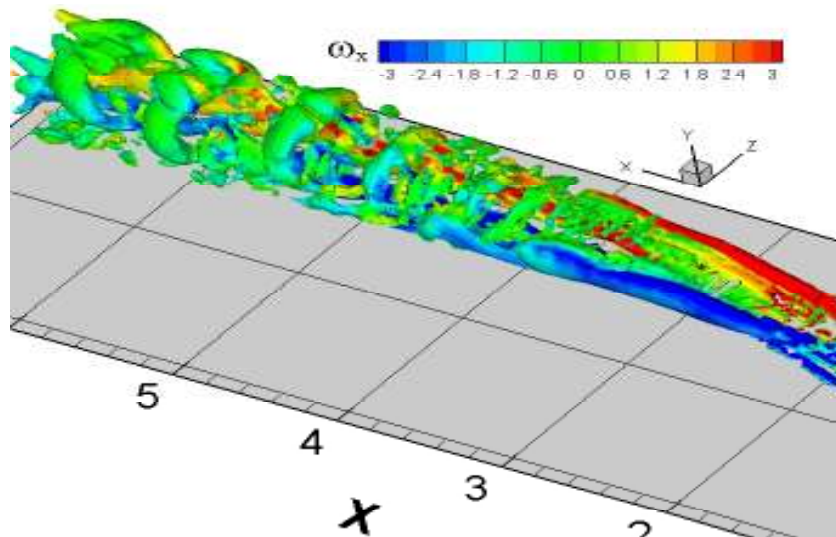


Figure 10. Hairpin vortices for inclined jet in cross flow (Laminar).

The primary structure appearing in the jet is a hairpin coherent structure. In the hairpin structure the two legs are aligned in the stream-wise direction with opposite vorticity, while the head of the structure is aligned with the span-wise direction. Parts of the legs, which join with the head, are in the wall normal direction.

When the same strategy for coherent structure identification is used with an instantaneous flow field from the turbulent simulation a somewhat similar, but more complex, structure arises in the flow, as shown in figure 11. In both figures iso-surfaces are filled with contours of stream-wise vorticity and these illustrate the motion of the structures.

The main structure in the turbulent jet is similar to what is observed for the laminar jet, i.e. a hairpin structure. There is a great deal of transient unsteady motion, which is due to turbulence, but the basic structure and evolution is similar. There are secondary stream-wise structures originating upstream. These structures are the main features of the wall turbulence.

These structures interact with each other and generate very complex features in the downstream wake region and explain features appearing in the instantaneous and average vorticity fields. In figure 7 a roller structure was identified which can be associated with a hairpin vortex. The first such structure in figure 7 appears between 3D and 4D downstream, which is clearly the head part of a vortex in figure 11 almost at the same location. The other random structures appearing along with the roller structures can be identified as stream-wise vortices, which are being trapped by the jet.

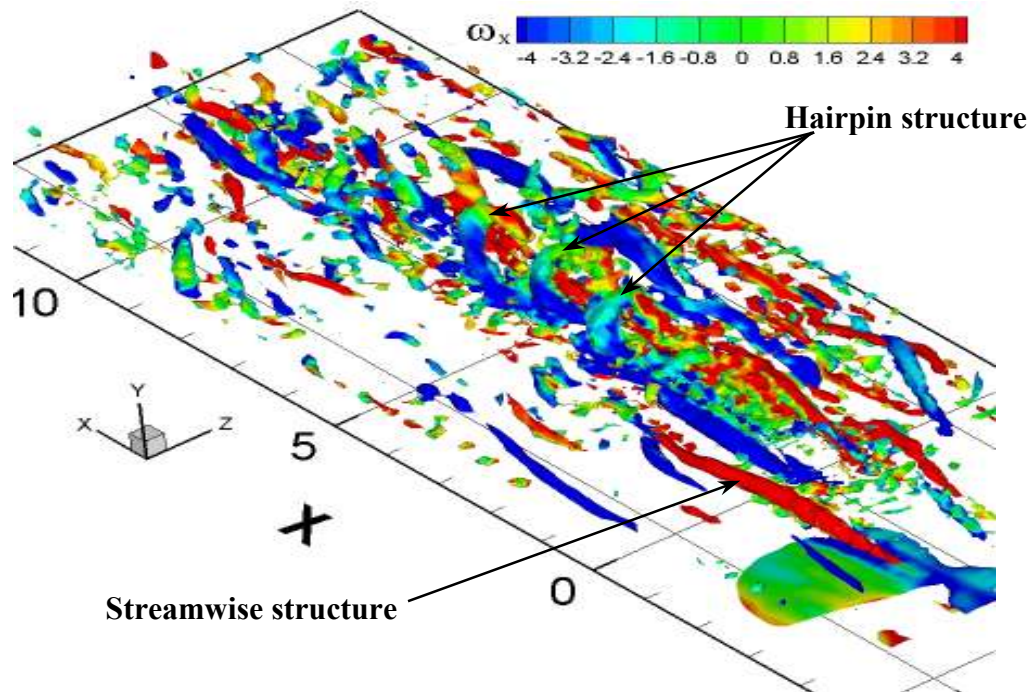


Figure 11. Coherent structures for inclined jet in cross flow (Turbulent).

The CVP in the average flow field is one of the main jet structures and can be correlated with the hairpin vortices or, more appropriately, with the legs of the hairpin

vortices. The hairpin vortices move with the flow but the legs fall on almost same position with the same vorticity sign on any given y-z plane. On averaging the flow field both legs provide two opposite sign vorticity regions on any given y-z plane which can be describe as CVP like in figure 6.

The stream-wise vortices contribute to the wall normal vorticity of figure 8. In the jet wake region both the hairpin vortices and the stream-wise vortices play a role. The elongated regions of vorticity represent legs of the hairpin, as well as the stream-wise vortices trapped by the jet. On the other hand, smaller spots of wall normal vorticity can be linked with the vertical part of the hairpin vortices.

Conclusions

A large eddy simulation has been performed for an inclined jet in a cross flow. The following conclusions may be made:

- It has been shown that various individual structures identified in the jet are related to single coherent structures.
- Near wall turbulence interacts with the jet and stream-wise vortices are trapped in the jet wake, which can have significant effect on scalar and heat transport.

References

1. Sargison, J. E., Guo, S. M., Oldfield, M. L. G., Lock, G. D. and Rawlinson, A. J., A converging slot-hole film-cooling geometry-Part 1: Low speed flat-plate heat transfer and loss, *ASME J. of Turbomachinery*, Vol. 124, 453-460 (2002).
2. Lee, S. W., Park, S. W. and Lee, J. S., Flow characteristics inside circular injection hole normally oriented to a cross flow: Part I- Flow visualizations and flow data in the symmetry plane, *ASME J. of Turbomachinery*, Vol. 123, 266-273 (2001).
3. Rowbury, D. A., Oldfield, M. L. G. and Lock, G. D., Large scale testing to validate the influence of external crossflow on the discharge coefficients of film cooling holes, *ASME J. of Turbomachinery*, Vol. 123, 593-600 (2001).
4. Gritsch, M., Schulz, A. and Wittig, S., Effect of crossflows on the discharge coefficient of film cooling holes with varying angles of inclination and orientation, *ASME J. of Turbomachinery*, Vol. 123, 781-787 (2001).
5. Lakehal, D., Theodoridis, G. S. and Rodi, W., Computation of film cooling of a flat plate by lateral injection from a row of holes, *Int. J. of Heat and Fluid Flow*, Vol. 19, 418-430 (1998).
6. Acharya, S., Tyagi, M. and Hoda, A, Flow and heat transfer predictions for film cooling, Heat transfer in gas turbine systems, *Ann. N.Y. Acad. Sci.*, Vol. 934, 110-125 (2001).
7. Medic, G. and Durbin P. A., Toward improved film cooling prediction, *ASME J. of Turbomachinery*, Vol. 124, 193-199 (2002).
8. Tyagi, M. and Acharya, S., Large eddy simulation of film cooling flow from an inclined cylindrical jet, *ASME J. of Turbomachinery*, Vol. 125, 734-742 (2003).
9. Moin, P. and Kim, J., Numerical investigation of turbulent channel flow, *J. Fluid Mech.*, Vol. 118, 341-377 (1982).

10. Zang, Y., Street, R. L. and Koseff, J. R., A dynamic mixed subgrid-scale model and its application to turbulent recirculating flows, *Phys. Fluids A*, Vol. 5(12), 3186-3196 (1993).
11. Swartztrauber P. N., A direct method for the discrete solution of separable elliptic equations. *SIAM J. Numer. Anal.*, Vol. 11, No. 6, 1136-1150 (Dec. 1974)
12. Yuan, L. L., Street, R. L. and Ferziger, J. H., Large-eddy simulations of a round jet in crossflow, *J. Fluid Mech.*, Vol. 379, 71-104 (1999).
13. Jin, G. and Braza M., A Nonreflecting outlet boundary condition for incompressible unsteady Navier-Stokes calculations, *J. Comp. Phys.*, Vol. 107, 239-253 (1993).
14. Fric, T. F. and Roshko A., Vortical structure in the wake of a transverse jet, *J. Fluid Mech.* Vol. 279,1-47 (1994).